Main linac lattice design and optimization for E_{cm}=1 TeV CLIC[*]

WANG Yi-Wei(王毅伟)[1;1)]   SCHULTE Daniel[2]   GAO Jie(高杰)[1]

[1] Institute of High Energy Physics, Chinese Academy of Sciences, Beijing 100049, China
[2] CERN, Geneva, Switzerland

Abstract: The Compact Linear Collider (CLIC) is a future e$^+$e$^-$ linear collider. The CLIC study concentrated on a design of center-of-mass energy of 3 TeV and demonstrated the feasibility of the technology. However, the physics also demands lower energy collision. To satisfy this, CLIC can be built in stages. The actual stages will depend on LHC results. Some specific scenarios of staged constructions have been shown in CLIC Concept Design Report (CDR). In this paper, we concentrate on the main linac lattice design for E_{cm}=1 TeV CLIC aiming to upgrade from E_{cm}=500 GeV CLIC and then to E_{cm}=3 TeV one. This main linac accelerates the electron or positron beam from 9 GeV to 500 GeV. A primary lattice design based on the 3 TeV CLIC main linac design and its optimization based on the beam dynamics study will be presented. As we use the same design principles as 3TeV CLIC main linac, this optimization is basically identical to the 3 TeV one. All the simulations results are obtained using the tracking code PLACET.

Key words: CLIC, main linac, lattice design, beam dynamics

PACS: 29.20.Ej, 41.85.-p, 41.75.Fr   **DOI:** 10.1088/1674-1137/38/6/067009

1 Introduction

The Compact Linear Collider (CLIC) is a future e$^+$e$^-$ linear collider. The CLIC study concentrated on a design of center-of-mass energy of 3 TeV and demonstrated the feasibility of the technology. However, the physics also demands lower energy collision. To satisfy this, CLIC can be built in stages. The actual stages will depend on LHC results. Some specific scenarios of staged constructions have been shown in CLIC Concept Design Report (CDR)[1]. In this paper, we concentrate on the main linac lattice design for E_{cm}=1 TeV CLIC aiming to upgrade from E_{cm}=500 GeV CLIC and then to E_{cm}=3 TeV one. This main linac accelerates the electron or positron beam from 9 GeV to 500 GeV. A primary lattice design based on the 3 TeV CLIC main linac design and its optimization based on the beam dynamics study will be presented. As we use the same design principles as 3 TeV CLIC main linac, this optimization is basically identical to the 3 TeV one. All the simulations results are obtained using the tracking code PLACET [4].

Consider the scenario that all stages of CLIC main linac are built with the 3 TeV CLIC accelerating structures whose gradient is 100 MV/m and working frequency 12 GHz. Beam parameters for the 1 TeV CLIC main linac are based on the 3 TeV CLIC design. See Table 1. This allows to reuse the main beam generation complex before main linac, the beam delivery system (BDS), main linac modules and the drive beam generation complex. The detailed account can be found in Ref. [1].

Table 1. Beam parameters for the main linac of 1 TeV CLIC.

parameters	value
initial energy E_0/GeV	9
final energy E_f/GeV	500
bunch population N_e	3.72×10^9
repetition rate f_{rep}/Hz	50
No. of bunches per pulse N_b	312
bunch spacing Δs/cm	15
bunch length σ_z/μm	44
initial rms energy spread $\left(\frac{\sigma_E}{E}\right)_0$(%)	$\leqslant 2$
final rms energy spread $\left(\frac{\sigma_E}{E}\right)_f$(%)	$\leqslant 0.35$
initial horizontal normalized emittance ϵ_{x0}/nm	$\leqslant 600$
final horizontal normalized emittance ϵ_{xf}/nm	$\leqslant 660$
initial vertical normalized emittance ϵ_{y0}/nm	$\leqslant 10$
final vertical normalized emittance ϵ_{yf}/nm	$\leqslant 20$

2 Lattice design

In CLIC, the RF power to accelerate the main beam is provided by the drive-beam decelerators which run parallel to the main linac. To facilitate the geometric match-

ing between drive beam decelerator and main linac, they are built using a chain of 2.01 m long two-beam modules [1]; The modules contain 8 accelerating structures or less structures and one quadrupole.

The main linac lattice is constructed with FODO cells and consists of several sectors. In each sector, the cell length and focal length are constant. The beta functions between different sectors are matched with last 3 quadrupoles of one sector and first 2 quadrupoles of its next sector. Along the whole main linac, the length of the half cell l and the focal length f have been chosen to scale as

$$l = l_0 \sqrt{\frac{E}{E_0}}, \quad f = f_0 \sqrt{\frac{E}{E_0}}, \quad (1)$$

in order to roughly obtain a beta function $\beta \propto \sqrt{E}$ [8], where E is the beam energy along the linac, l_0 is the initial half cell length, f_0 is the initial focal length and E_0 is the initial beam energy. This scaling allows to maintain roughly constant phase advance per cell μ along the whole main linac:

$$\mu = 2 \arcsin\left(\frac{l_0}{2f_0}\right). \quad (2)$$

The choice for 3 TeV CLIC main linac is: $l_0 = 1.5$ m, $f_0 = 1.3$ m [8]. This corresponds to $f_0/l_0 \approx 0.9$ and $\mu = 70.5°$. A primary design for 1 TeV CLIC main linac can be obtained immediately by shortening the 3 TeV one. Fig. 1 shows the vertical beta function.

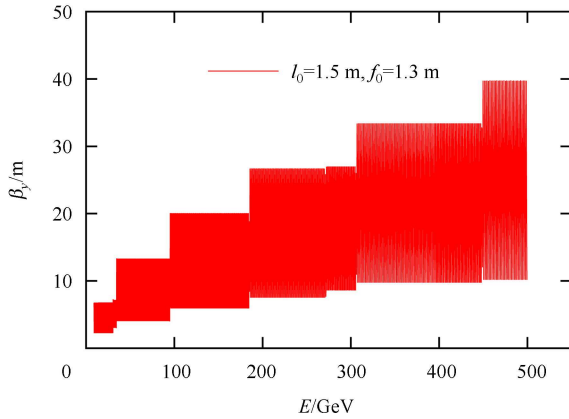Fig. 1. The vertical beta function along the main linac (for the lattice: $l_0 = 1.5$ m, $f_0 = 1.3$ m).

A strong focusing lattice will reduce the wakefield effect while increases dispersive effects and vice versa. To balance these two effects, we should carefully choose the initial half cell length l_0 and focal length f_0 based on the beam dynamics study. In main linac, many kinds of imperfections can lead to normalized emittance growth (In the following, the emittance always means the normalized one.) by the dispersion and wakefield effects.

They can be classified into static and dynamic ones. The static imperfections include the errors of reference line, elements to reference line and so on; The dynamic imperfections include beam jitter, ground motion, element jitter and so on. For CLIC main linac, the budgets of static imperfections are 30 nm (5%) and 5nm (50%) for the horizontal and vertical plane respectively; The budgets of dynamic imperfections are 30 nm (5%) and 5 nm (50%) for the horizontal and vertical plane respectively as well. We will limit our discussion to the vertical plane as the budgets for the horizontal plane are easy to be fulfilled.

Besides the performance (mainly emittance growth), the cost should also be considered when optimizing the lattice. We can use the quadrupole fill factor η_Q (defined as quadrupole length l_Q over half cell length l) to denote the cost of the lattice. The scaling laws of Eq. (1) lead to roughly constant η_Q along the whole main linac:

$$l_Q \approx \frac{1}{kf} = \frac{1}{\dfrac{B'}{B\rho}f} \propto \frac{\sqrt{E}}{f_0} \Rightarrow \eta_Q \equiv \frac{l_Q}{l} \propto \frac{1}{f_0 l_0} = \frac{1}{\left(\dfrac{f_0}{l_0}\right)l_0^2}. \quad (3)$$

where k, B' and $B\rho$ are the quadrupole strength, quadrupole field gradient and the magnetic rigidity respectively. Thus, a smaller η_Q means shorter total length of quadrupoles thus a cheaper machine. In the following, we will use the value of η_Q obtained from the real lattices but not the scaling law of Eq. (3) which just to show the scaling.

3 Beam stability and BNS damping

The initial beam jitter will exponentially amplified by the transverse wakefield. To stabilize the beam, the BNS damping [2] is used. In this scheme, a correlated energy spread is introduced along the bunch such that the tail has a lower energy than the head by manipulating the RF phase. Consider two-particle wakefield model where the head macro-particle has the design energy E and the tail one has an energy spread $\Delta E/E$. The transverse position difference can be corrected if energy spread

$$\Delta E/E = -\beta_0^2 \frac{N_e e^2 W_\perp(2\sigma_z)}{2E_0}, \quad (4)$$

introduced [6], where β_0 is the initial beta function, e is the electron charge, $W_\perp(z)$ is the transverse wakefield function and the other parameters are shown in Table 1.

In CLIC, the beam is accelerated with a small RF phase ϕ_{RF} in most of main linac and a large phase 30 degree in the last part to take out the energy spread. usually, a larger energy spread is better for beam stability. Figs. 2 and 3 show the result for the primary lattice: $l_0 = 1.5$ m, $f_0 = 1.3$ m. In this paper, we will just keep $\phi_{RF} = 8°$ for the first stage.
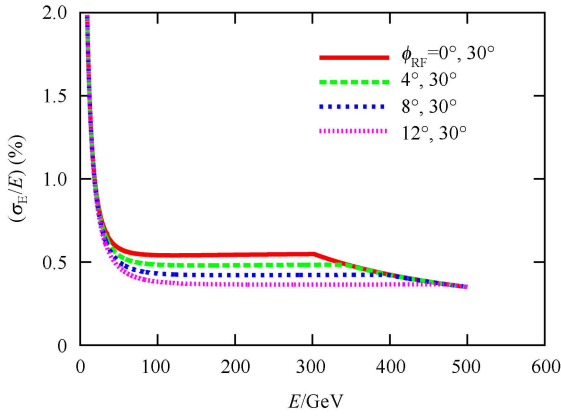
Fig. 2.   The rms energy spread along the main linac (for the lattice: $l_0 = 1.5$ m, $f_0 = 1.3$ m).
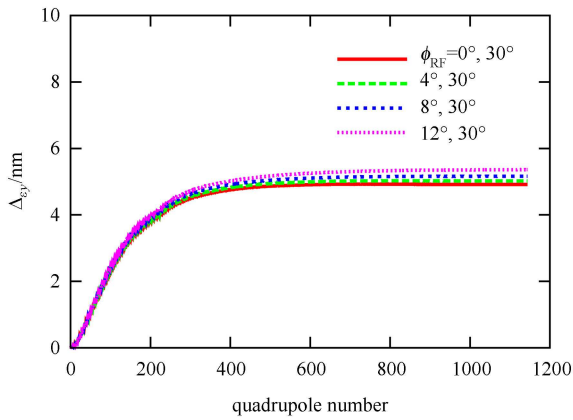

Fig. 3.   The vertical emittance growth with BNS damping for an initial beam jitter of one σ_{y0} (for the lattice: $l_0 = 1.5$ m, $f_0 = 1.3$ m).

3.1   Optimization of lattice strength

Considering dispersion effect only, the emittance growth due to initial beam jitter can be estimated as (assume the beam fully filaments) [9]

$$(\Delta\varepsilon_y)_{\mathrm{disp}} = \frac{1}{2}\frac{y_0^2}{\beta_{y0}} = \frac{1}{2}\epsilon_y\left(\frac{y_0}{\sigma_{y0}}\right)^2, \qquad (5)$$

where y_0 is position of initial beam jitter, β_{y0} is the initial beta function, ϵ_y is the initial emittance and σ_{y0} is the initial beam size. For the initial beam jitter of one σ_{y0}, this emittance growth is 5 nm. We normalize the emittance growth $\Delta\varepsilon_y$ due to initial beam jitter with the one considering dispersion effect only $(\Delta\varepsilon_y)_{\mathrm{disp}}$. We choose the stable lattices whose $\Delta\varepsilon_y/(\Delta\varepsilon_y)_{\mathrm{disp}}$ smaller than 1.2. See Fig. 4.

The upper figure of Fig. 4 shows that a strong focusing lattice with small l_0 and f_0/l_0 is good for BNS damping. This is only from the view point of lattice performance.

Considering the cost of lattice as well, the lower figure of Fig. 4 shows that we can use larger l_0 and rather small f_0/l_0 to have good BNS damping with little space lost to quadrupoles. This corresponds to a larger phase advance per cell.
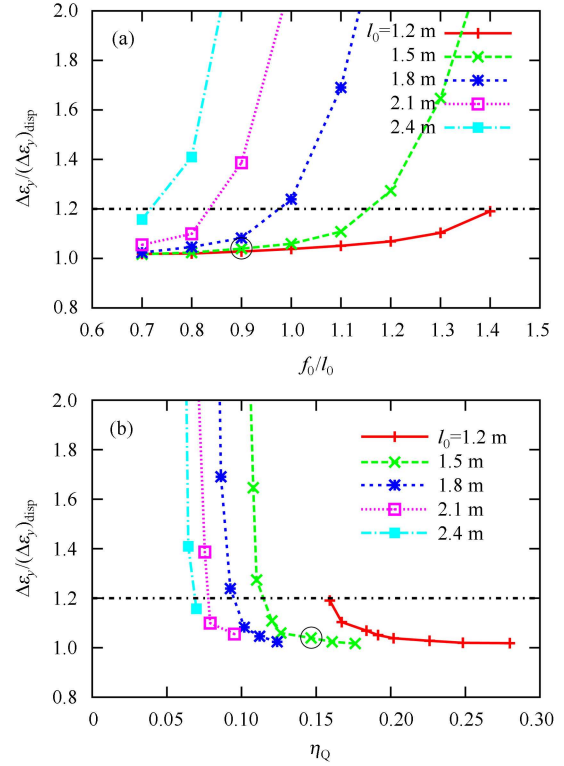

Fig. 4.   The vertical emittance growth with BNS damping for the initial beam jitter. The point in a black circle corresponds to the lattice with $(l_0, f_0/l_0) = (1.5$ m$, 0.9)$ which can be looked as the primary lattice. (a): as a function of f_0/l_0. (b): as a function of quadrupole fill factor quadrupole fill factor η_{Q}.

3.2   Bunch population limit

For the stable lattices which have been chosen, we try to get their bunch population limits. Firstly, we get the shortest possible bunch length σ_z for a bunch population N_{e} to reduce the transverse wakefield effects from the following conditions:

1) Fix the average RF phase $\overline{\phi_{\mathrm{RF}}} = 12°$ along the main linac;

2) Fix final energy $E_{\mathrm{f}}(G_{\mathrm{act}}, \overline{\phi_{\mathrm{RF}}}, N_{\mathrm{e}}, \sigma_z) = 500$ GeV;

3) Limit the final rms energy spread $\left(\dfrac{\sigma_E}{E}\right)_{\mathrm{f}}(G_{\mathrm{act}},$

$\overline{\phi_{\mathrm{RF}}}, N_{\mathrm{e}}, \sigma_z) \leqslant 0.35\%$ which mainly from the BDS and physics requirements [1, 6];

where G_{act} is the actural accelerating gradient determined by the conditions. The bunch length is a linear function of bunch population. See Fig. 5. Then, we get their bunch population limits by increasing the bunch

population until the beam is unstable, i.e., $\Delta\varepsilon_y/(\Delta\varepsilon_y)_{\mathrm{disp}}$ equal to 1.2. The bunch population limit of the primary lattice is about 4.5×10^9. See Fig. 6. A large bunch population limit corresponds to small emittance growth and vice versa. Thus, this again favors a larger l_0 and rather small f_0/l_0. Later, we will use the value of bunch population limit to present the performance of beam stability.
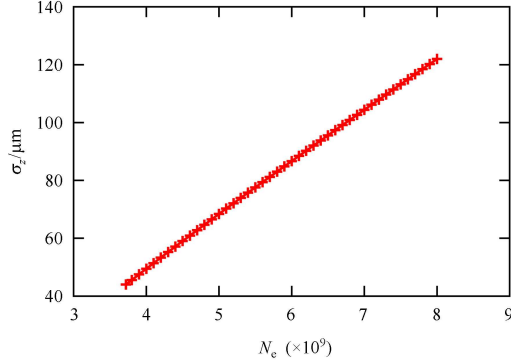

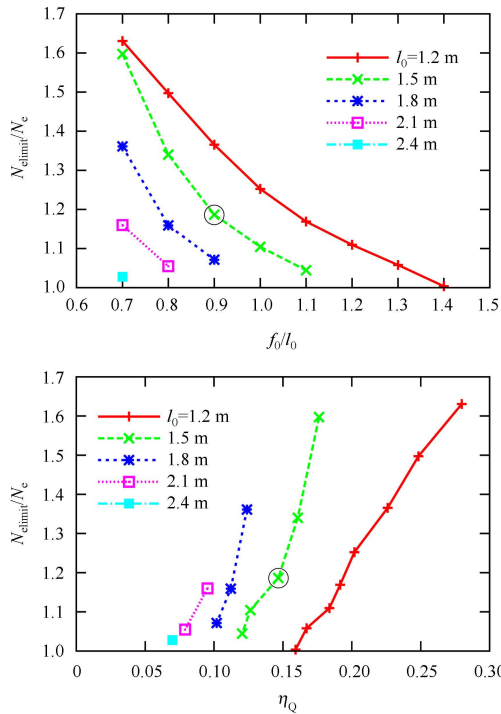Fig. 5. The bunch length as a function of bunch population.

Fig. 6. The bunch population limit for the stable lattices. The nominal bunch population $N_e = 3.72\times10^9$.

4 Static imperfections

In CLIC main linac, all the components are mounted on movable girders. The beam position monitor (BPM)

and quadrupole and mounted on a common support which can be moved independently of the girder. Each girder is linked to the next girder forming an articulation point [3], see Fig. 7.
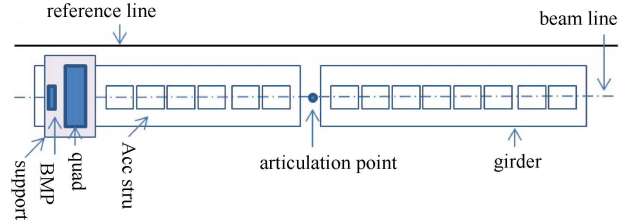

Fig. 7. The alignment model of CLIC main linac.

The static imperfections could be sorted to local and global one. The local imperfections are assumed that the reference line is straight along the whole main linac. In this paper, we just consider local imperfection as usually their tolerances are much stricter than the global one [3]. Table 2 shows the local static imperfections and their values after pre-alignment [1] which are the same as 3 TeV CLIC main linac. To preserve the emittance in CLIC main linac, three beam-based alignments called one-to-one (1-2-1) correction, dispersion free steering (DFS) and wake free steering (WFS) are performed in order [3].
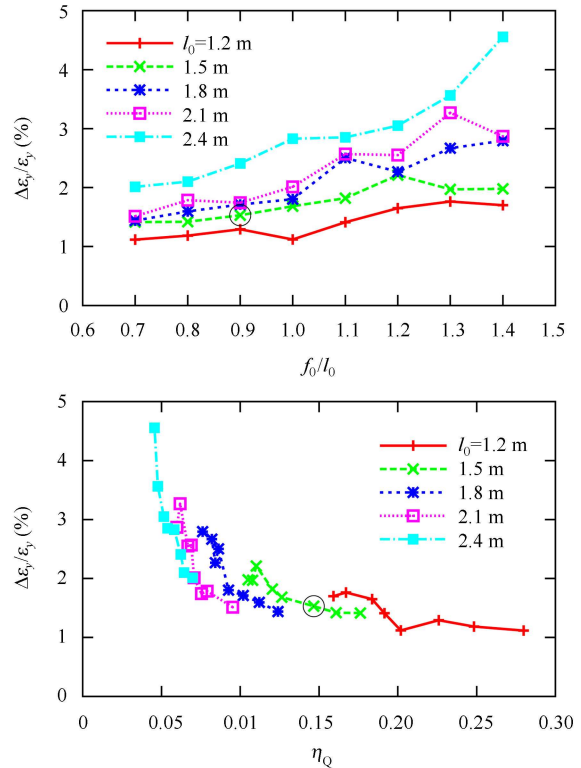

Fig. 8. The vertical emittance growth after beam-based alignment for wake monitor offset.

Table 2.   The vertical emittance growth due to static imperfections with the lattice $l_0=1.5$ m, $f_0=1.3$ m.

| imperfection	with respect to	value	WFS/nm	DFS/nm	1-2-1/nm	no correction/nm
BPM offset	wire reference	14 μm	0.131	9.554	420.822	—
BPM resolution	—	0.1 μm	0.021	0.818	—	—
accelerating structure offset	girder axis	10 μm	0.006	1.222	1.227	1.972
accelerating structure tilt	girder axis	140 μrad	0.222	0.256	0.068	1265.929
articulation point offset	wire reference	10 μm	0.027	7.150	7.180	14.468
girder end point	articulation point	5 μm	0.006	1.073	1.076	6.189
wake monitor	structure center	3.5 μm	0.135	—	—	—
quadrupole roll	longitudinal axis	100 μrad	0.065	0.065	0.065	0.065
all	—	—	0.590	18.499	423.558	5819276.751
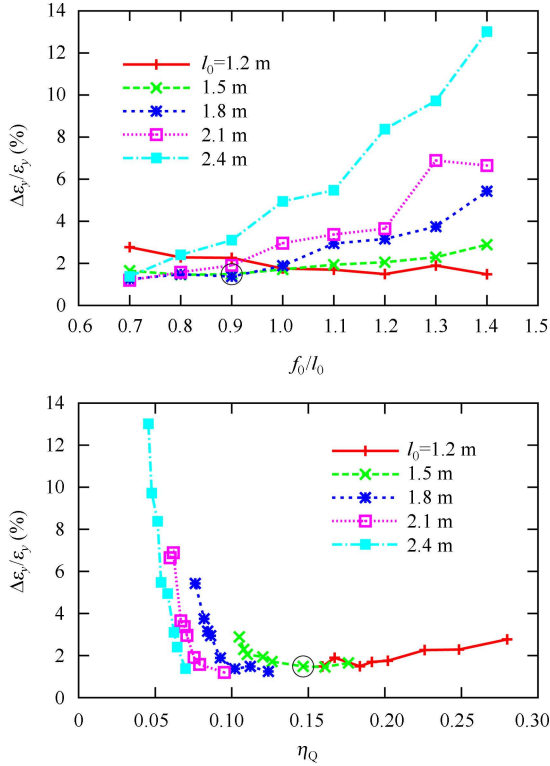
Fig. 9.   The vertical emittance growth after beam-based alignment for BPM offset.

4.1   Primary lattice

Firstly, we track for the primary design whose initial half cell and focal length are $l_0=1.5$ m and $f_0=1.3$ m. After the beam-based alignments, the relative emittance growth of single bunch is about 6% which is very small. See Table 2.

4.2   Lattice optimization

Firstly, we study the emittance growth due to the wake monitor and BPM offset separately with different lattices.

As the wake monitor offset after WFS actually lead to accelerating structure offset, wakefield effect is dominate in this case. Thus, a strong focusing lattice with small

l_0 and f_0/l_0 will have a good preservation of emittance growth. The emittance growth $\Delta\varepsilon_y$ is roughly proportional to the average beta function of initial cell $\overline{\beta_{y0}}$[6]:

$$\Delta\varepsilon_y \propto \overline{\beta_{y0}} \approx l_0 \frac{\left(\frac{2f_0}{l_0}\right)^2}{\sqrt{\left(\frac{2f_0}{l_0}\right)^2 - 1}}. \tag{6}$$

See upper figure of Fig. 8.

The BPM offset after 1-2-1 correction and DFS actually lead to slightly quadrupole offset, and then lead to accelerating structure offset after WFS. The wakefield effect is also dominate in this case unless a very strong focusing lattice. See upper figure of Fig. 9.
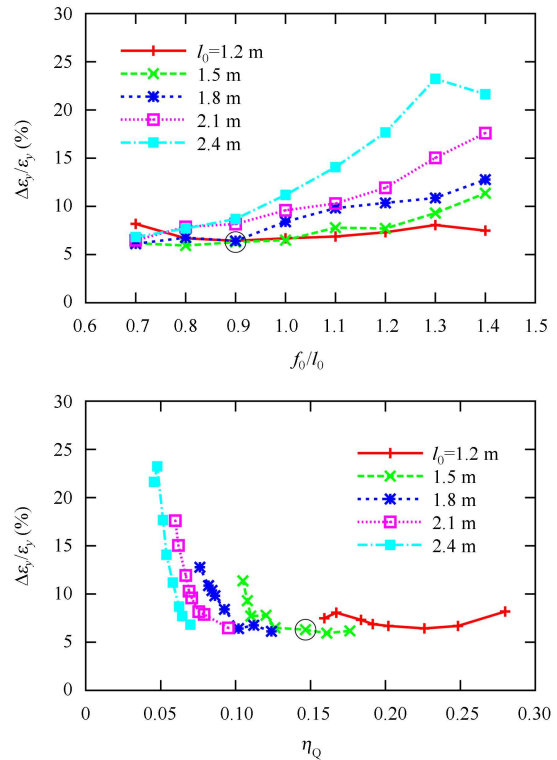

Fig. 10.   The vertical emittance growth after beam-based alignment for all the static imperfections listed in Table 2.

Then, we study the emittance growth due to all the imperfections listed in Table 2. The wakefield effect is still dominate in this case. See upper figure of Fig. 10.

The lower figures of Figs. 8, 9 and 10 show that we can use larger l_0 and rather small f_0/l_0 to have good beam-based alignment with little space lost to quadrupoles.

5   Dynamic imperfections

5.1   Ground motion

After some time, the corrected linac will be affected by ground motion leading to more emittance growth. Considering low frequency (<0.1 Hz) vibration, the relative RMS motion Δ of two points with distance L after time T can be described by ATL law [5]:

$$\Delta^2 = ATL. \tag{7}$$

The constant A depends on the site of the linac and 0.5×10^{-6} $\mu m^2/sm$ is chosen here [1]. This model is a simplification to be able to give an estimate on the expected effect from ground motion.
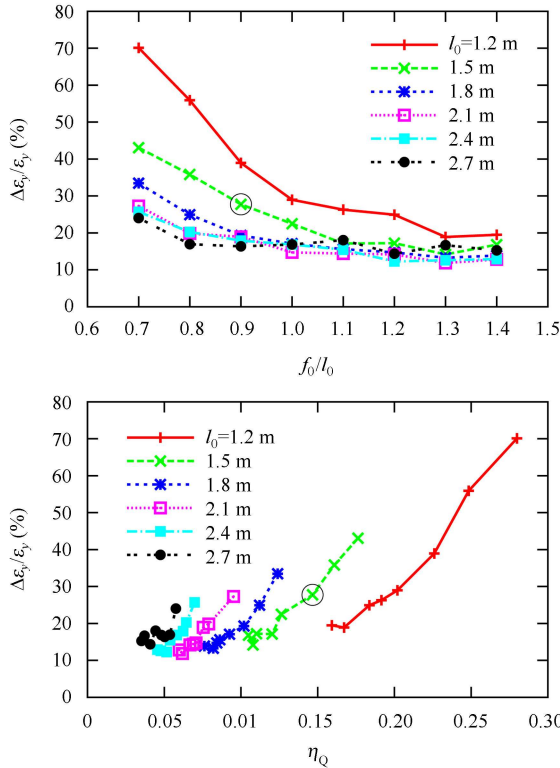

Fig. 11.   The vertical emittance growth for ground motion after 1-2-1 correction ($T=10^6$ s, without residual static imperfection).

We study the vertical emittance growth due to ground motion without the residual static imperfection.

We set $T=10^6$ s (12 days) and apply 1-2-1 correction which can be done in feedback mode. After the 1-2-1 correction, the vertical emittance growth has been well controlled. See upper figure of Fig. 11. Large l_0 and f_0/l_0 lead to small emittance growth as dispersion effect is dominate for the lattices we simulated. Even weaker focusing will lead to a smaller emittance growth but less beam stability.

The lower figure of Fig. 11 shows that we can use larger l_0 and large f_0/l_0 to have good emittance preservation with very samll quadrupole fill factor η_Q.

5.2   Quadrupole jitter

The quadrupole jitter is also an important dynamic imperfection. Many reasons such as the rapid ground motion, mechanical vibration can lead to quadrupole jitter. In CLIC, the stability of the vertical quadrupole position is nm scale which is very strict.

The quadrupole jitter will lead to beam jitter at the end of main linac thus dilute the multi-pulse emittance. Considering a point bunch model, the relative vertical position jitter due to quadrupole jitter can be estimate as [6]

$$\frac{\langle \Delta y_{\mathrm{f}}^2 \rangle}{\sigma_{y_{\mathrm{f}}}^2} \propto \frac{y_{\mathrm{q}}^2}{l_0^2 \sqrt{\left(\frac{2f_0}{l_0}\right)^2 - 1}}, \tag{8}$$

where Δy_{f} is the final vertical position of beam, $\sigma_{y_{\mathrm{f}}}$ is the final vertical beam size and y_{q} is rms vertical position of quadrupole. Large l_0 and f_0/l_0, i.e., weak focusing lead to a small position jitter. The simulation result is shown in Fig. 12. The multi-pulse emittance growth can be estimated as [6]

$$\frac{\Delta \varepsilon_y}{\varepsilon_y} \propto \frac{\langle \Delta y_{\mathrm{f}}^2 \rangle}{\sigma_{y_{\mathrm{f}}}^2}. \tag{9}$$
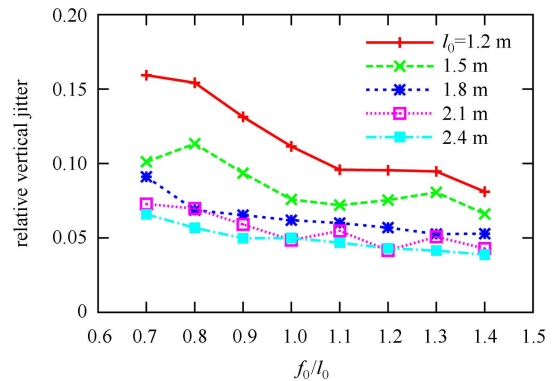

Fig. 12.   The relative vertical position jitter due to quadrupole jitter $y_{\mathrm{q}}=1$ nm (point bunch).
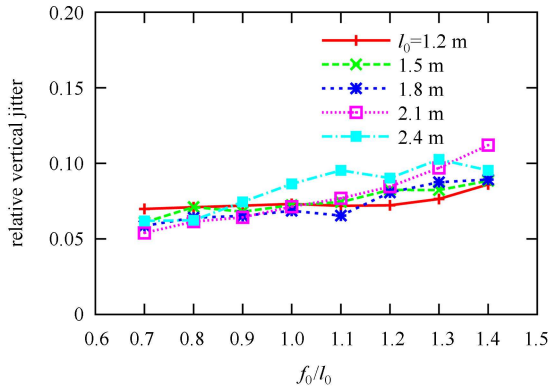
Fig. 13.   The relative vertical position jitter due to quadrupole jitter $y_q = 1$ nm (realistic bunch).

For a realistic bunch, the wakefield and dispersion effects make quite different results. See the Fig. 13. If we go to much weaker or much stronger focusing region, the trends of the results should be the same as the point bunch case.

Figure 14 shows the emittance growth due to the quadrupole jitter. we can use larger l_0 and rather small f_0/l_0 to have good emittance preservation with little space lost to quadrupoles.
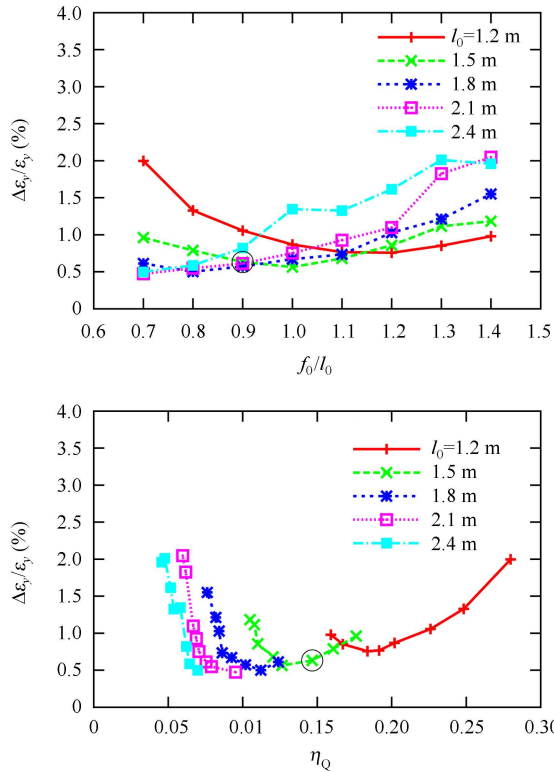

Fig. 14.   The vertical emittance growth due to quadrupole jitter $y_q = 1$ nm (realistic bunch).

6   Lattice choice

We make our lattice choice firstly by balancing the performance considering beam stability, static imperfections after beam-based alignment, ground motion after 1-2-1 correction and quadrupole jitter. Then the cost is considered.

Figures 15, 16 and 17 shows the vertical emittance growth for the static imperfections after beam-based alignment, ground motion after 1-2-1 correction and quadrupole jitter vs. the bunch population limit for beam stability respectively. The length of the bar indicates the quadrupole fill factor η_Q of a lattice. We get the lattices well balancing the performance of the four cases by choosing the common lattices in the frames (i.e., lattices with small emittance growth and large bunch population limit). Then we drop the cases whose quadrupole fill factors η_Q are obviously higher (more expensive) than the other cases. We get the lattices shown in Table 3. A
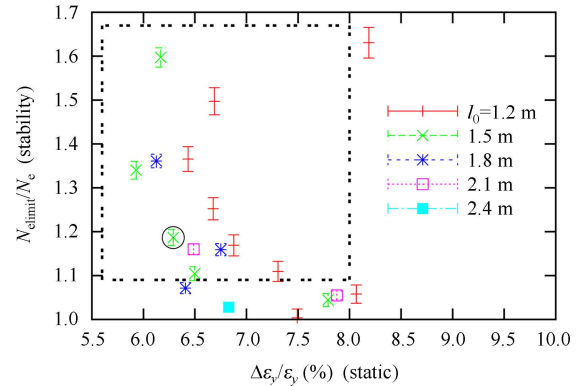

Fig. 15.   The vertical emittance growth for the static imperfections after beam-based alignments vs. the bunch population limit for the beam stability with BNS damping.
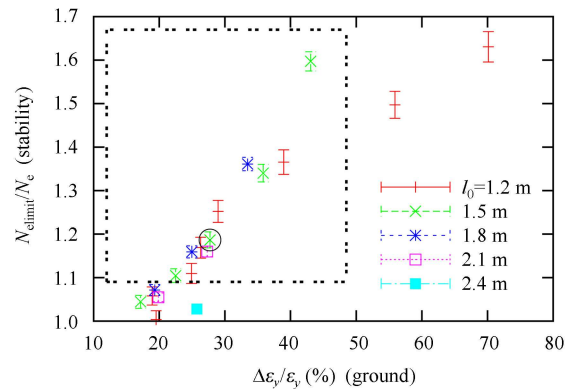

Fig. 16.   The vertical emittance growth for the ground motion after 1-2-1 correction vs. the bunch population limit for the beam stability with BNS damping.

Table 3.   Lattices well balancing the performance and cost.

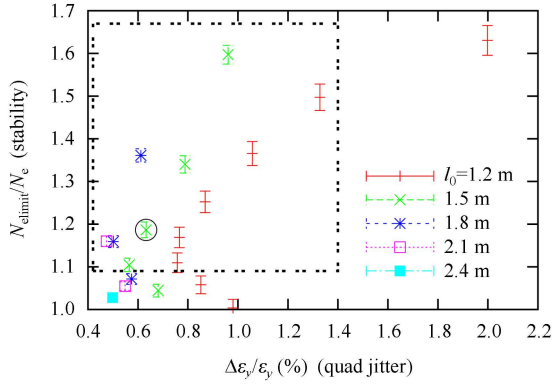| case	l_0/m	f_0/l_0	$N_{\mathrm{elimit}}/N_{\mathrm{e}}$	$\Delta\epsilon_y/\epsilon_y(\%)$(static)	$\Delta\epsilon_y/\epsilon_y(\%)$(ground)	$\Delta\epsilon_y/\epsilon_y(\%)$(quad)	η_{Q}
1	1.5	0.9	1.19	6.29	27.7	0.63	0.147
2	1.5	1.0	1.10	6.50	22.5	0.56	0.126
3	1.8	0.7	1.36	6.12	33.5	0.61	0.124
4	1.8	0.8	1.16	6.75	25.0	0.50	0.112
5	2.1	0.7	1.16	6.49	27.3	0.47	0.095

Fig. 17.   The vertical emittance growth for the quadrupole jitter vs. the bunch population limit for the beam stability with BNS damping.

final choice of the lattices will depend on carefully balancing between the performance and the cost. Thus we conclude that the lattices with $(l_0,\ f_0/l_0)$ around (1.5 m, 0.9), (1.5 m, 1.0), (1.8 m, 0.7), (1.8 m, 0.8) and (2.1 m, 0.7) can be chosen as optimized lattices with the 3 TeV CLIC accelerating structures. Note that the primary choice (1.5 m, 1.3/1.5) is included in our optimized choices.

7   Conclusions and further work

The main linac design of E_{cm}=1 TeV CLIC with E_{cm}=3 TeV CLIC accelerating structures has been presented here. We give a primary design by shortening the original 3 TeV CLIC main linac and the optimization of the lattice based on the beam dynamics study. As we use the same design principles as 3 TeV CLIC main linac, this optimization is basically identical for the 3 TeV CLIC main linac.

Firstly, we studied the beam instability due to initial beam jitter and its control by BNS damping. Then we studied the emittance growth due to kinds of static imperfections and the corrections by beam-based alignments. We also studied two main dynamic imperfections: ground motion and quadrupole jitter; To control the emittance growth due to the ground motion, we do the 1-2-1 correction in feedback mode. Finally, by balancing the performance and considering cost of the lattices, we conclude that the lattices with $(l_0,\ f_0/l_0)$ around (1.5 m, 0.9), (1.5 m, 1.0), (1.8 m, 0.7), (1.8 m, 0.8) and (2.1 m, 0.7) can be chosen as optimized lattices with the 3 TeV CLIC accelerating structures. Note that the primary choice (1.5 m, 1.3/1.5) is included in our optimized choices.

In CLIC, wakefield induced multi-bunch effects are important. With the 3 TeV accelerating structure, the long-range wake field of each bunch applies a kick to the next following bunch and the field amplitude is 6.6 kV/pCm^2 [7]. The multi-bunch effects of the optimized lattices are undergoing.

References

1 Aicheler M, Burrows P, Draper M et al. CLIC Conceptual Design Report, CERN-2012-007
2 Balakin V, Novakhatsky A, Smirnow V. Proc. of 12th Int. Conf. on High Energy Accelerators, Fermilab, 1983
3 Schulte D. Beam-Based Alignment in the New CILC Main Linac, CLIC-Note-804
4 Latina A et al. Recent Improvements in the Tracking Code PLACET. Proc. of 11th biennial European Particle Accelerator Conference, Genoa, Italy, 2008
5 Baklakov B A et al. Proc. of IEEE Particle Accelerator Conf.,
San Francisco, USA, 1991. 3273–3275
6 Schulte D. The Lectures on Main Linac. 5th Linear Collider School. 2010
7 Schulte D. Multi-Bunch Calculations in the CLIC Main Linac, CLIC-Note-805
8 Schulte D. Emittance Preservation in the Main Linac of CLIC. Proc. 23rd IEEE Particle Accelerator Conf., Vancouver, Canada. 2009. 3808–3810
9 Raubenheimer Tor O. The Generation and Acceleration of Low-Emittance Flat Beams for Future Linear Collider (Ph.D. thesis). Stanford University, 1992, Chapter 3.4.1.1